SLITs Suppress Tumor Growth *In vivo* by Silencing *Sdf1/Cxcr4* within Breast Epithelium

Rebecca Marlow,[1] Phyllis Strickland,[1] Ji Shin Lee,[3] Xinyan Wu,[3] Milana PeBenito,[1] Mikhail Binnewies,[1] Elizabeth K. Le,[1] Angel Moran,[1] Hector Macias,[1] Robert D. Cardiff,[2] Saraswati Sukumar,[3] and Lindsay Hinck[1]

[1]Department of Molecular, Cell and Developmental Biology, University of California, Santa Cruz, California; [2]University of California Davis Center of Comparative Medicine, Davis, California; and [3]Sidney Kimmel Comprehensive Cancer Center, Johns Hopkins University School of Medicine, Baltimore, Maryland

Abstract

The genes encoding *Slits* and their *Robo* receptors are silenced in many types of cancer, including breast, suggesting a role for this signaling pathway in suppressing tumorigenesis. The molecular mechanism underlying these tumor-suppressive effects has not been delineated. Here, we show that loss of *Slits*, or their *Robo1* receptor, in murine mammary gland or human breast carcinoma cells results in coordinate up-regulation of the *Sdf1* and *Cxcr4* signaling axis, specifically within mammary epithelium. This is accompanied by hyperplastic changes in cells and desmoplastic alterations in the surrounding stroma. A similar inverse correlation between *Slit* and *Cxcr4* expression is identified in human breast tumor tissues. Furthermore, we show in a xenograft model that *Slit* overexpression down-regulates CXCR4 and dominantly suppresses tumor growth. These studies classify *Slits* as negative regulators of *Sdf1* and *Cxcr4* and identify a molecular signature in hyperplastic breast lesions that signifies inappropriate up-regulation of key prometastatic genes. [Cancer Res 2008;68(19):7819–27]

Introduction

The multistep model for breast carcinogenesis postulates that invasive carcinoma arises by way of intermediate hyperplastic lesions that progress in severity through stages of atypia to *in situ* and finally invasive carcinoma. It is generally recognized that there are clinically significant differences between various hyperplastic lesions, with some containing cellular and molecular changes that confer higher risk of progression to invasive disease. Pathologists identify clinically relevant differences later in disease progression, but early breast lesions are not well defined and further subclassification of their tumor potential by morphologic criteria is likely to be impossible. Consequently, assessing the potential risks associated with premalignant breast disease will rely on refining our understanding of the molecular signatures that confer increased risk of progression from epithelial hyperplasia to invasive carcinoma.

Up-regulation of CXCR4 is an example of one molecular change in breast cancer cells that is associated with poor prognosis (1, 2). Its role in directing metastasizing breast cancer cells to target sites is well established (3). Little is known, however, about the role of CXCR4 during breast cancer progression, although it is up-regulated early during cellular transformation (1, 4), along with SDF1 (5), which is produced by cancer-associated fibroblasts (CAF) and is in the local environment (6, 7). Recent studies have identified roles for this signaling pathway in primary breast tumors (8, 9), and in this context, one possibility is that signaling through the CXCR4/SDF1 axis drives proliferation, conferring selective advantage to cells as they transform into metastasizing carcinomas. Several mechanisms up-regulate CXCR4 during tumor metastasis (10–13), but there is little information about mechanisms regulating the SDF1/CXCR4 chemokine axis in organs at early stages of transformation.

SLITs (*Slit1, Slit2*, and *Slit3*) are a family of secreted proteins that mediate positional interactions between cells and their environment during development by signaling through ROBO receptors (*Robo1, Robo2, Robo3*, and *Robo4*; ref. 14). SLIT/ROBO signaling, however, is not restricted to development, and loss of these cues likely plays an important role during tumor progression. *Slits* and *Robos* are considered candidate tumor suppressor genes because their promoters are frequently hypermethylated in epithelial cancers (15–18). In ~50% of sampled human breast tumors, *Slit2* or *Slit3* gene expression is silenced (15, 19).

Cross-talk between SLIT/ROBO and CXCR4/SDF1 signaling has been observed in several systems, with the regulatory effect occurring downstream of the receptors and involving modulation of intracellular signaling intermediates. In leukocytes and human breast cancer cell lines, SLIT impedes SDF1-induced chemotaxis (20, 21). In breast cancer cells, this deterring effect occurs via SLIT-mediated inhibition of SDF1-induced activation of signaling pathways involved in motility (21). Similarly, in the nervous system, a reciprocal regulation of SLIT-mediated axonal repulsion by SDF1 is exerted through modulation of cyclic nucleotide signaling intermediates (22). These studies show an intriguing interrelationship between these signaling axes but do not address the consequences of losing the function of one of these signaling systems, such as occurs in breast during tumor progression when *Slit* expression is silenced.

Here, we investigate the consequences of losing SLIT/ROBO1 signaling in murine mammary gland, human breast cancer cells, and human tumors. We identify *Sdf1* and *Cxcr4* as critical targets of SLIT/ROBO1 regulation. Exploiting the ability to transplant knockout mammary epithelium into host mammary fat pads, we determine the compartment, epithelial or stromal, in which SLIT/ROBO1 signaling occurs, and how loss of signaling in one location leads to alterations across the epithelial/stromal boundary. Finally, we explore the tumor-suppressive capabilities of *Slits* using a xenograft model of human breast cancer.

Note: Supplementary data for this article are available at Cancer Research Online (http://cancerres.aacrjournals.org/).

R. Marlow and P. Strickland contributed equally to this work.

Requests for reprints: Lindsay Hinck, Department of Molecular, Cell and Developmental Biology, University of California, Santa Cruz, CA 95064. Phone: 831-459-5253; Fax: 831-459-3139; E-mail: hinck@biology.ucsc.edu.

doi:10.1158/0008-5472.CAN-08-1357

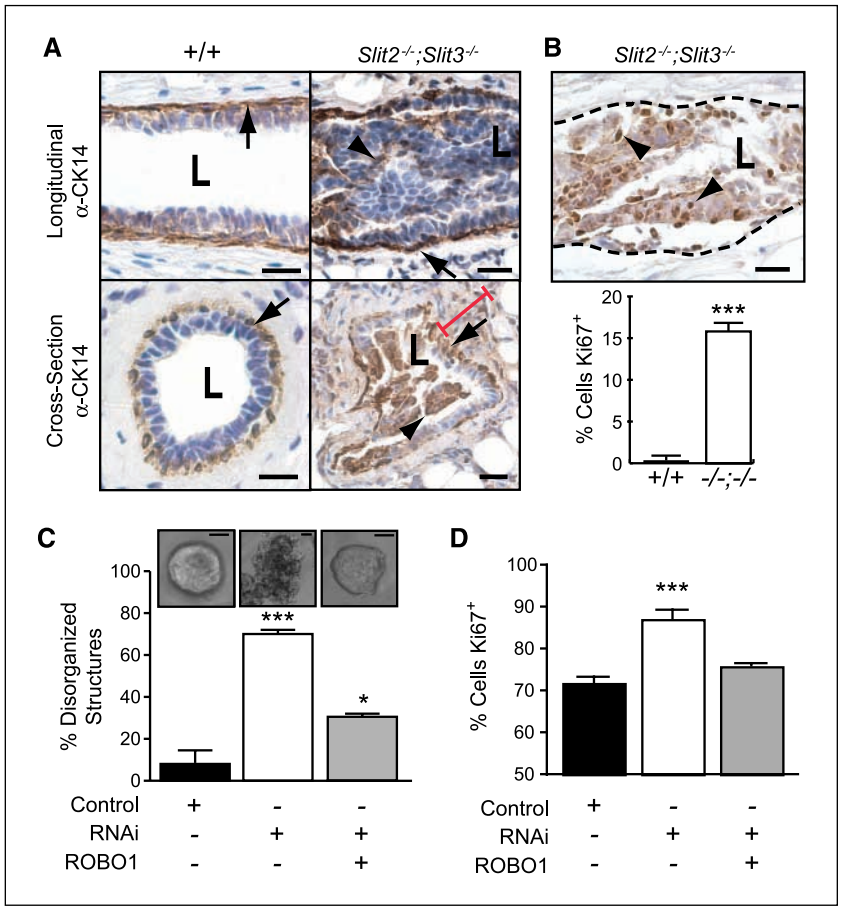

Figure 1. Loss of *Slit2* and *Slit3* expression in mammary epithelium leads to the formation of hyperplastic disorganized lesions. *A,* lack of SLIT in the epithelium leads to lesion formation. Immunostaining with anti-CK14 on longitudinal sections and cross-sections through +/+ and *Slit2*$^{-/-}$;*Slit3*$^{-/-}$ mammary outgrowths. *Arrows,* ductal myoepithelial cell layer; *arrowheads,* CK14-positive cells abnormally located in the lumen. *Red bar,* condensed desmoplastic stroma. *L*, lumen. *B,* lack of SLIT leads to hyperplasia. Representative lesion with dashed line indicating epithelial/stromal interface. *Arrowheads,* Ki67^{+} cells. *Columns,* mean percentage [n = 3 animals at 12 wk of age, 15 fields of view/animal (5×)]; *bars,* SD. ***, $P < 0.0001$, unpaired t test. *C,* lack of ROBO1 leads to a disorganized phenotype in three-dimensional culture. After transfection, MCF7 cells were grown in Matrigel. After 5 d, colonies were photographed (5×) and percentage of disorganized structures was counted. Representative images of colonies are shown. *Scale bar,* 10 μm. *Columns,* mean percentage; *bars,* SD. ***, $P < 0.0001$, ANOVA. *RNAi,* RNA interference. *D,* lack of ROBO1 increases the cell proliferation index. *Columns,* mean percentage of Ki67^{+} cells; *bars,* SD. **, $P < 0.001$, ANOVA.

Materials and Methods

Clinical samples. Frozen or formalin-fixed paraffin-embedded tissue specimens were collected at Johns Hopkins University (Baltimore, MD). All human tissue was collected using protocols approved by the Institutional Review Board. Informed consent was obtained from each individual who provided tissue linked with clinical data.

Animals. The study conformed to guidelines set by University of California at Santa Cruz animal care committee (Chancellor's Animal Research Committee). Mouse Slit2, Slit3, and Robo1 nulls were generated and genotyped as described (23).

Transplant techniques. Mammary anlage was rescued from E16-20 embryos and transplanted into precleared fat pads of athymic nude mice (24). Tissue fragments from the resulting outgrowths were contralaterally transplanted to generate knockout and wild-type tissue controls (25).

Implantation of Elvax beads. Elvax, an ethylene vinyl copolymer capable of sustained slow release of bioactive molecules, was prepared as described (26), with pellets containing 225 ng SDF1 and 0.45 mg bovine serum albumin (BSA) for control. Pellets were contralaterally implanted into the fat pad of wild-type CD1 mice (n = 3), and tissue was harvested after 6 d.

Cell lines, DNA constructs, and antibodies. MCF7 and MDA-MB-231 cells were maintained in DMEM supplemented with 10% FCS. pGL-CXCR4(−375) contains CXCR4 between −357 and +51 relative to the transcription site followed by the luciferase gene (12). pCRII-SDF1 (for riboprobes) contains 538-nucleotide fragment of the mouse *Sdf1* cDNA (27). Mouse image clone 3385804 (American Type Culture Collection). Small interfering RNA (siRNA) directed against *Robo1* was from Santa Cruz Biotechnology. pSecTagB-*hSlit3*-C-myc was from Dr. Roy Bicknell (University of Birmingham, Birmingham, United Kingdom). The following antibodies were used: anti-CK14 (AF64, Covance), anti-SMA (1A4, Sigma), anti-Ki67 (Santa Cruz Biotechnology), anti-CXCR4 (Abcam), anti-SDF1 (Santa Cruz Biotechnology), anti-SLIT3 (Chemicon), anti-SLIT2 (Chemicon), anti-HA (Dr. Doug Kellog, University of California, Santa Cruz, CA), anti-Myc (9E10), anti-ROBO1 (Abcam), and anti-extracellular signal-regulated kinase (Santa Cruz Biotechnology).

Generation of stable cell lines. MDA-MB-231 cells were transfected with pSecTagB-Slit2-HA and pSecTagB-Slit3-Myc and selected in zeocin (Invitrogen). n = 3 lines were generated expressing SLIT2-HA and n = 2 lines expressing SLIT3-Myc.

Tumor generation. Stable cell lines (10^6 cells) were injected into precleared fat pads of nude mice. Tumor volume was calculated using the formula $(\text{length} \times \text{width})^2/2$.

Immunohistochemistry. Tissue was fixed in 4% paraformaldehyde. Paraffin-embedded tissue was sectioned at 6 μm and serially mounted. Standard protocols were used and avidin-biotin complex method (Vector Labs) was used for amplification.

Scoring of immunohistochemistry. Immunostaining was scored according to percentage positive cells (P) and staining intensity (I). Score equals P + I. P scores 0 (none), 1 (<1%), 2 (1–10%), 3 (10–30%), 4 (30–60%), and 5 (>60%). I scores 0 (none), 1 (weak), 2 (intermediate), and 3 (strong).

siRNA transfection. MCF7 cells were transiently transfected using *Robo1* siRNA (Santa Cruz Biotechnology) and Lipofectamine 2000 (Invitrogen) according to the manufacturers' instructions. For three-dimensional culture, the "on-top" method was used (28). For luciferase assay, 48 h before harvest, cells were cotransfected with pGL-CXCR4(−375) (F-luciferase) and pRL-TK (R-luciferase). Cells were lysed using passive lysis buffer and assay was carried out in triplicate using the Dual-Luciferase Assay System (Promega) and Wallac Victor Luminometer (Perkin-Elmer Life Sciences) according to the manufacturers' instructions. F-luciferase activity was normalized to R-luciferase activity (transfection efficiency).

Western blotting. Western blotting was performed using standard procedures (29). Band intensity was scanned using Typhoon 9410 imager and quantified using ImageQuant 5 software.

Quantitative real-time reverse transcription-PCR analysis. Real-time reverse transcription-PCR (RT-PCR) analysis was done as previously described (30). Data were first analyzed using the Sequence Detector Software SDS 2.0 (Applied Biosystems). Results were calculated and normalized relative to glyceraldehyde-3-phosphate dehydrogenase (GAPDH) control. All of the PCR assays were done in triplicate, and mean values are shown in figures.

***In situ* hybridization.** *In situ* hybridization was carried out as described previously (23, 25).

Primary cell isolation. Primary mammary epithelial cells were prepared from mild collagenase and dispase digestion, as described (23). Cells were plated overnight and then trypsinized and placed onto Matrigel-coated coverslips.

Chemotaxis assay. Chemotaxis was examined as described before (29). Phase-contrast images were acquired at 0 and 60 min. The change in cell area in the directed quadrant was calculated using ImageJ.

Statistical analysis. We used factorial design ANOVA, unpaired t tests, or Mann-Whitney tests to analyze data as appropriate. Significant ANOVA values were subsequently subjected to post-test using the Tukey-Kramer comparison. We report P values for each statistical test; all P values were <0.05.

Results

Loss of *Slit* or *Robo1* in mammary epithelium leads to the formation of hyperplastic, disorganized lesions. Given the expanding role of SLITs in epithelial biology, we hypothesized a tumor-suppressive function for *Slits* in breast. We previously showed that two *Slit* family members, *Slit2* and *Slit3*, are expressed in murine mammary gland (23). The homozygous *Slit2*$^{-/-}$ mutation causes perinatal lethality. Therefore, to investigate the consequence of its loss in mature mammary gland, we generated *Slit2*$^{-/-}$;*Slit3*$^{-/-}$ outgrowths by contralateral transplantation of knockout and wild-type anlage into cleared fat pads of immunocompromised mice (24).

We examined mature *Slit2*$^{-/-}$;*Slit3*$^{-/-}$ mammary outgrowths for morphology. Compared with the open lumens and organized bilayers of ducts in control outgrowths, *Slit2*$^{-/-}$;*Slit3*$^{-/-}$ ducts displayed striking abnormalities (Fig. 1*A*). The phenotype was 100% penetrant, with ~30% of ducts having lesions extending between 0.3 and 5.0 mm. We categorized the lesions as mild and severe. Mild lesions contained cells in the luminal space (10.1% ± SE 1.9; n = 621 ducts; 5 outgrowths), and many of these cells were peeled away from the myoepithelial layer, similar to an adhesive defect previously described in *Ntn1*$^{-/-}$;*Slit2*$^{-/-}$ glands (23). In severe lesions (17.8% ± SE 8.1; n = 621 ducts; 5 outgrowths), ductal lumens were occluded with a disorganized mass of cells (Fig. 1*A*). These excess cells suggested disrupted growth control due to either increased proliferation and/or decreased apoptosis. We labeled proliferating cells and observed a significant increase in the percentage of Ki67^{+} cells in *Slit2*$^{-/-}$;*Slit3*$^{-/-}$, compared with +/+, ducts (Fig. 1*B*). This increase is responsible for the excess cells

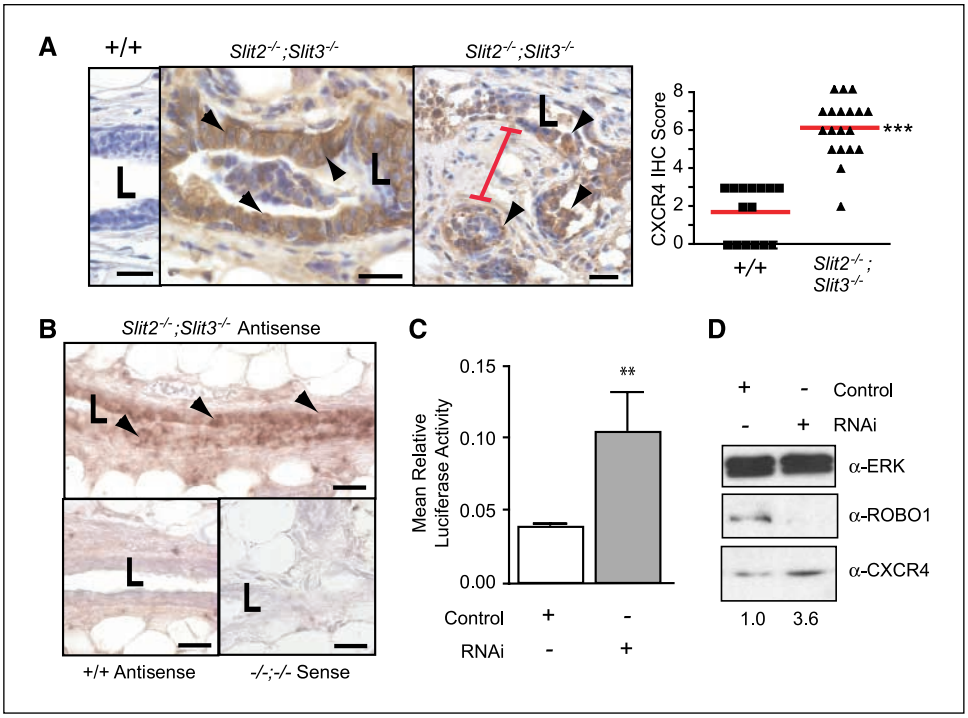

Figure 2. Loss of *Slit2* and *Slit3* causes up-regulation of CXCR4 in mouse mammary gland and human MCF7 cells. *A,* in *Slit2*$^{-/-}$;*Slit3*$^{-/-}$ outgrowths, CXCR4 protein expression is localized to epithelia, with desmoplastic stroma between lesions. Representative immunostaining with anti-CXCR4 on +/+ and *Slit2*$^{-/-}$;*Slit3*$^{-/-}$ mammary outgrowths. *Arrowheads,* positive epithelial cells. *Red bar,* condensed desmoplastic stroma. *Scale bar,* 20 μm. CXCR4 immunostaining was scored according to positivity and staining intensity and plotted on a vertical scatter plot. *Red bars,* average score. Significantly more CXCR4 staining is seen in *Slit2*$^{-/-}$;*Slit3*$^{-/-}$ outgrowths. ***, P < 0.0001, Mann-Whitney. *B, Cxcr4* mRNA is specifically present in the epithelium of *Slit2*$^{-/-}$;*Slit3*$^{-/-}$ outgrowths. *In situ* hybridization on +/+ and *Slit2*$^{-/-}$;*Slit3*$^{-/-}$ outgrowths using antisense probes reveals *Cxcr4* mRNA in *Slit2*$^{-/-}$;*Slit3*$^{-/-}$, but not +/+, cells. *Arrowheads,* positive epithelial cells. Sense probes show little or no background staining. *Scale bar,* 20 μm. *L,* lumen. *C,* loss of SLIT/ROBO signaling in MCF7 cells leads to up-regulation of *Cxcr4* gene expression. Cells were treated with control or *Robo1* siRNA and then cotransfected with pGL-CXCR4(−375), which contains the *Cxcr4* promoter region coupled to the F-luciferase gene and pRL-TK (R-luciferase). Cells were lysed after 36 h and luciferase activity was measured in triplicate. Activities were normalized for transfection efficiency. *Columns,* mean relative luciferase activity; *bars,* SE. **, P = 0.0095, Mann-Whitney test. *D,* loss of SLIT/ROBO signaling in MCF7 cells leads to increased levels of CXCR4 protein. Representative immunoblots (n = 4). *Numbers,* CXCR4 band intensity.

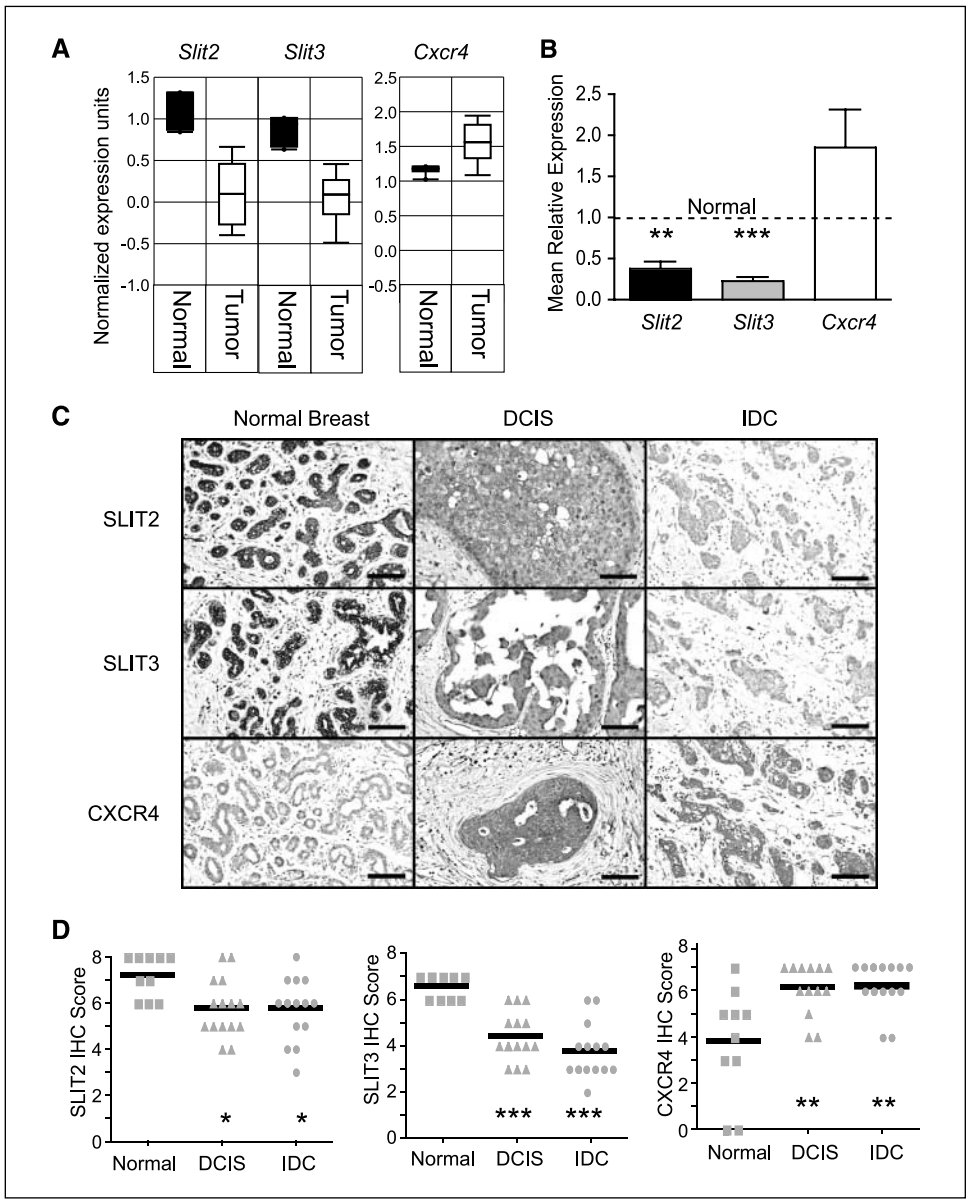

Figure 3. Loss of *Slit* expression in human tumors correlates with up-regulation of *Cxcr4*. *A,* box plots of data from the Richardson microarray data set were drawn using the Oncomine Cancer Profiling Database (32). *Slit2* ($P = 2.6E{-}10$) and *Slit3* ($P = 7.1E{-}9$) expression is significantly reduced in tumors, whereas *Cxcr4* ($P = 1.8E{-}5$) expression is elevated. Normal, $n = 7$; tumor, $n = 40$; P values from t test. *B,* expression levels, by quantitative PCR, of *Slit2, Slit3*, and *Cxcr4* were obtained from a panel of tumors, with values normalized against internal control *GAPDH*. The data were then normalized to values obtained from normal breast ($n = 6$). A value of 1 equals expression level of the gene in average normal breast. Seventeen of 25 tumor samples (68%) showed elevated *Cxcr4* expression compared with normal breast. In these tumors, this elevation corresponded with significantly reduced expression of *Slit2* or *Slit3*. *Columns,* mean relative expression; *bars,* SE. *Slit2* versus *Cxcr4*: **, $P < 0.011$; *Slit3* versus *Cxcr4*: ***, $P < 0.001$, ANOVA. *C,* SLIT expression is decreased in tumors, whereas CXCR4 levels increase. Normal breast, DCIS, and IDC tissue sections were immunostained with anti-SLIT2, anti-SLIT3, and anti-CXCR4. Representative images are shown. *Scale bar,* 100 μm. *D,* immunostained sections were scored according to cell percentage positivity and staining intensity. Scores were plotted on a vertical scatter plot. *Black bars,* average score. Both SLIT2 (*, $P = 0.01$, ANOVA) and SLIT3 (***, $P < 0.0001$, ANOVA) exhibit decreased expression in DCIS and IDC compared with normal breast. In contrast, CXCR4 is expressed at very low levels in normal breast, but its expression increases in DCIS and IDC (**, $P = 0.0005$, ANOVA).

because we evaluated apoptosis using activated caspase-3 staining and observed no difference (data not shown). Histopathologic analyses concurred with our observations that *Slit2*$^{-/-}$;*Slit3*$^{-/-}$ tissue contains hyperplasias. Condensed and desmoplastic stroma surrounding the lesions were also noted in the diagnosis (Fig. 1*A*), as was a large influx of immune infiltrates in the knockout, compared with wild-type, tissue.

ROBO1 is a SLIT receptor that could mediate the observed effects in the gland (23). *Robo1*$^{-/-}$ animals are viable so we evaluated the loss-of-function phenotype using intact glands. Ducts in *Robo1*$^{-/-}$ glands were hyperplastic and disorganized, displaying a phenotype that was indistinguishable from *Slit2*$^{-/-}$;*Slit3*$^{-/-}$ ductal lesions (Supplementary Fig. S1). As was the case for *Slit2*$^{-/-}$;*Slit3*$^{-/-}$ tissue, the penetrance of the phenotype was 100%, with ~30% of ducts displaying lesions that extended between 0.3 and 5.0 mm.

To investigate whether a similar phenotype occurred when SLIT/ROBO1 signaling was disrupted in human breast cells, we used the MCF7 line that retains several characteristics of differentiated mammary epithelium, including expression of *Slit2, Slit3*, and *Robo1* (data not shown; ref. 31). Cells were treated with *Robo1* siRNA to down-regulate SLIT/ROBO1 signaling (Supplementary Fig. S2) and then cultured in Matrigel. MCF7 cells formed smooth, nonpolarized colonies without central lumens. In contrast, the siRNA-treated colonies were large and disorganized, a phenotype that was rescued by reexpression of *Robo1* (Fig. 1*C*). Immunostaining with Ki67 revealed a significantly higher fraction of proliferating cells in colonies treated with *Robo1* siRNA compared with control (Fig. 1*D*). This was similar to the elevated proliferation observed in *Slit2*$^{-/-}$;*Slit3*$^{-/-}$ outgrowths and *Robo1*$^{-/-}$ glands (Fig. 1*B*; Supplementary Fig. S2). Together, these data show that a consequence of *Slit/Robo1* loss is elevated proliferation leading to hyperplastic lesions.

Loss of *Slit* up-regulates *Cxcr4* expression. We sought candidates whose misexpression in the absence of SLIT/ROBO1 signaling is responsible for the observed hyperplastic phenotype.

One candidate is CXCR4 because it is expressed early during breast tumorigenesis (1, 4), and blocking its expression or function inhibits breast tumor growth (8, 9). Western blots of whole gland lysates showed elevated CXCR4 expression in *Slit2*$^{-/-}$;*Slit3*$^{-/-}$, compared with +/+, tissue (Supplementary Fig. S3). Immunohistochemistry revealed CXCR4 expression in a large fraction of cells in *Slit2*$^{-/-}$;*Slit3*$^{-/-}$ epithelium, with little or no expression in +/+ epithelium (Fig. 2*A*). We also observed condensed and desmoplastic stroma surrounding these CXCR4-positive lesions (Fig. 2*A*). Because CXCR4 is regulated by transcriptional and posttranscriptional mechanisms, we performed *in situ* hybridization studies and observed *Cxcr4* in *Slit* knockout, but not wild-type, epithelium (Fig. 2*B*). A transcriptional mechanism also occurred in *Robo1* siRNA-treated MCF7 cells because we observed increased *Cxcr4*

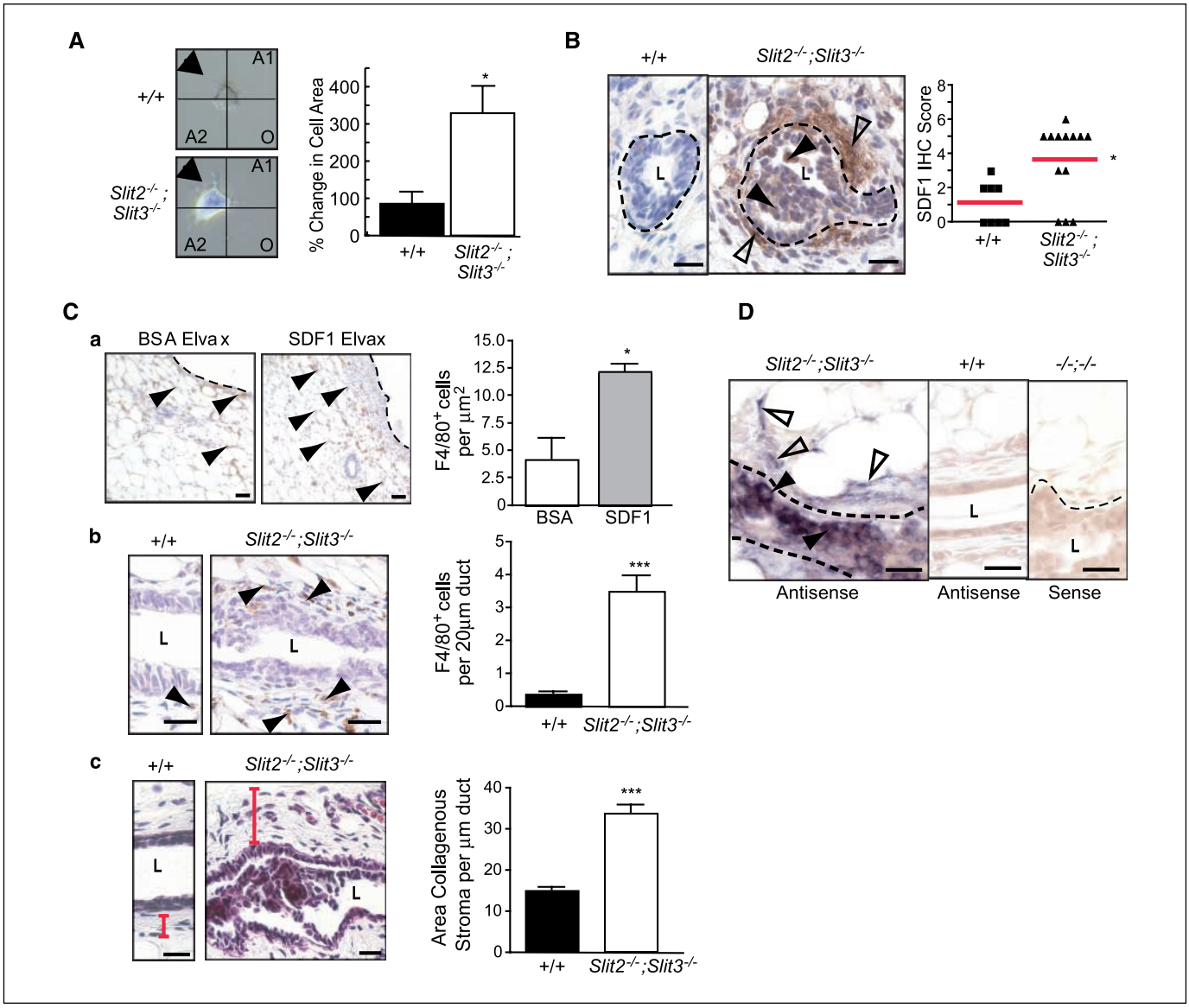

Figure 4. Loss of *Slit* expression results in coordinate up-regulation of SDF1 and the formation of desmoplastic stroma. *A, Slit2*$^{-/-}$;*Slit3*$^{-/-}$, but not +/+, cells respond to a point source of SDF1. Primary epithelial cells were prepared from outgrowths and placed in stable liquid gradients of SDF1 (29). Phase-contrast images were acquired at 0 and 60 min. Using ImageJ, the change in cell area in the source quadrant (*arrow*) was calculated. *Columns,* mean percentage change ($n = 7$); *bars,* SE. *, $P = 0.0018$, Mann-Whitney. *B,* SDF1 protein is present in the stroma surrounding *Slit2*$^{-/-}$;*Slit3*$^{-/-}$ outgrowths. Representative immunostaining with anti-SDF1 on +/+ and *Slit2*$^{-/-}$;*Slit3*$^{-/-}$ mammary outgrowths. *Dotted lines,* epithelial/stromal interface. *Open arrowheads,* positive staining in stroma; *arrowheads,* epithelial cells expressing SDF1. *Scale bar,* 20 μm. SDF1 immunostaining was scored according to positivity and intensity. Scores were plotted on a vertical scatter plot. *Red bars,* average score. Significantly more SDF1 staining is seen in *Slit2*$^{-/-}$;*Slit3*$^{-/-}$ outgrowths. *, $P = 0.018$, Mann-Whitney. *C,* SDF1 attracts macrophages. *a,* representative images of F4/80 staining in fat pads containing BSA versus SDF1 Elvax pellets. The number of F4/80$^+$ cells surrounding pellets was counted and expressed as the number of F4/80$^+$ cells per μm^2. *Columns,* average; *bars,* SD. *, $P = 0.0086$, unpaired *t* test. Macrophages surround *Slit2*$^{-/-}$;*Slit3*$^{-/-}$ ducts. *b,* representative images of F4/80 staining in +/+ versus *Slit2*$^{-/-}$;*Slit3*$^{-/-}$ tissue. Duct length was measured and the number of F4/80$^+$ cells was counted (ImageJ software). *Columns,* average; *bars,* SD. ***, $P < 0.0001$, unpaired *t* test ($n = 3$ animals, 10 fields of view/animal). Stroma surrounding *Slit2*$^{-/-}$;*Slit3*$^{-/-}$ ducts is desmoplastic. *c,* representative images of Masson's trichrome staining of +/+ versus *Slit2*$^{-/-}$;*Slit3*$^{-/-}$ tissue. *Red bar,* width of stroma. Longitudinal images of ducts were taken and duct length and positively stained areas were measured (ImageJ software). *Columns,* average; *bars,* SD. ***, $P < 0.0001$, unpaired *t* test. *Scale bar,* 20 μm. *D, Sdf1* mRNA is specifically present in subpopulations of elongated stromal cells (*open arrowheads*) and epithelial cells (*closed arrowheads*) in *Slit2*$^{-/-}$;*Slit3*$^{-/-}$ outgrowths. *In situ* hybridization on +/+ and *Slit2*$^{-/-}$;*Slit3*$^{-/-}$ outgrowths using antisense probes reveals *Sdf1* mRNA in *Slit2*$^{-/-}$;*Slit3*$^{-/-}$, but not +/+, cells. Sense probes show no or little background staining. *Scale bar,* 20 μm.

reporter gene activity and increased levels of CXCR4 in treated, compared with control, cells (Fig. 2*C* and *D*). Together, our results show that SLIT/ROBO1 signaling negatively regulates *Cxcr4* expression, with loss of this regulation leading to elevated levels of CXCR4 in murine tissue and human breast cancer cells.

If *Slits* silence *Cxcr4* in normal breast, we hypothesize that loss of *Slits* in tumors will correspond with elevated *Cxcr4.* To investigate, we analyzed microarray data sets from human breast tumor samples available at Oncomine.org (32) and found an inverse correlation between *Slit* and *Cxcr4* expression (Fig. 3*A*). We confirmed this by performing quantitative RT-PCR on a panel of human tumors; in 68% of tumors with elevated *Cxcr4* expression, *Slit2* or *Slit3* levels were significantly reduced compared with their expression in normal tissue (Fig. 3*B*). We further verified these observations at the protein level using immunohistochemistry on samples of normal breast, ductal carcinoma *in situ* (DCIS), and infiltrating ductal carcinoma (IDC; Fig. 3*C* and *D*). Again, there were robust levels of SLIT2 and SLIT3 in normal tissue that significantly decreased with increasing tumor grade. In contrast, and as previously shown (1, 4), little or no CXCR4 was detectable in normal breast, but its expression significantly increased with higher tumor grade.

Loss of *Slit* expression results in coordinate up-regulation of SDF1. Although CXCR4 is up-regulated in the vast majority of sampled premalignant lesions, studies on human breast cancer cell lines have suggested that it is only active in metastatic cells (33). To evaluate CXCR4 activity in *Slit2*$^{-/-}$;*Slit3*$^{-/-}$ cells, we performed chemotaxis assays. *Slit2*$^{-/-}$;*Slit3*$^{-/-}$ cells did not exhibit robust migration as expected of primary cells harvested from premalignant tissue but instead responded to SDF1 by reorganizing their cell membrane and sending membranous projections toward a point source (Fig. 4*A*). Wild-type cells were unresponsive to SDF1. This result suggested that CXCR4 expressed on *Slit2*$^{-/-}$;*Slit3*$^{-/-}$ cells is active and reacts to its ligand.

This raised the question of whether SDF1 surrounded *Slit2*$^{-/-}$;*Slit3*$^{-/-}$ lesions because recent studies have placed it in the tumor microenvironment (6, 7). We found abundant SDF1 expression in the epithelium and the surrounding stroma of knockout, but not wild-type, tissue (Fig. 4*B*). The presence of SDF1 is consistent with the histopathologic diagnosis that noted the infiltration of immune cells within desmoplastic stroma surrounding *Slit2*$^{-/-}$;*Slit3*$^{-/-}$ lesions. Macrophages, which express CXCR4, represent a major component of immune infiltrates surrounding tumors and play a key role in promoting the angiogenic switch during malignant transition (34). To determine whether macrophages are attracted to SDF1, we implanted point sources of SDF1 or vehicle (BSA) into wild-type mammary glands (Fig. 4*C, a*). Significantly more macrophages (F4/80^{+}) infiltrated into the tissue surrounding SDF1, compared with control, showing that SDF1 is a chemoattractant for macrophages and suggesting a role in recruiting these immune cells to tumors (Fig. 4*C, a*). Next, we

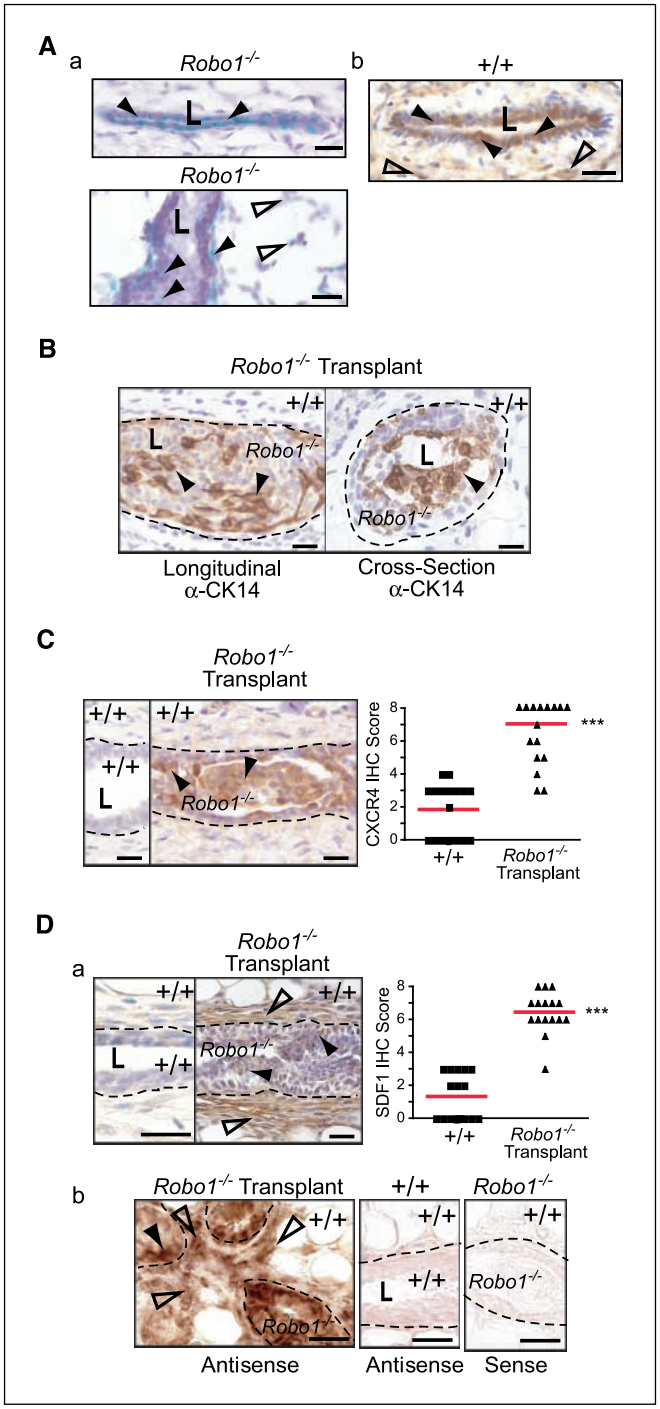

Figure 5. Coordinate up-regulation of CXCR4 and SDF1 is due to lack of SLIT/ROBO1 signaling within mammary epithelia. *A,* to examine *Robo1* gene expression, we took advantage of the *lacZ* gene under the control of the endogenous *Robo1* promoter in −/− tissue. *a,* longitudinal sections of *Robo1*$^{-/-}$ ducts stained for β-galactosidase activity. *b,* longitudinal section of +/+ duct immunostained with anti-ROBO1. *Open arrows,* positive stromal staining; *arrowheads,* positive epithelial cells. *Scale bar,* 20 μm. *L*, lumen. *B,* transplanted *Robo1*$^{-/-}$ mammary outgrowths show severe ductal defects similar to those observed in *Slit2*$^{-/-}$;*Slit3*$^{-/-}$ outgrowths. *Scale bar,* 20 μm. *C,* CXCR4 protein is specifically expressed in the epithelium of *Robo1*$^{-/-}$ outgrowths. Representative immunostaining with anti-CXCR4 on +/+ stroma/+/+ epithelia and +/+ stroma/*Robo1*$^{-/-}$ epithelia. *Arrows,* positive cells. *Scale bar,* 20 μm. CXCR4 immunostaining was scored and plotted on a vertical scatter plot. *Red bars,* average score. Significantly more CXCR4 staining is seen in *Robo1*$^{-/-}$ outgrowths. ***, $P < 0.0001$, Mann-Whitney test. *D,* SDF1 is present in the stroma surrounding *Robo1*$^{-/-}$ epithelial outgrowths (*a*; *open arrowheads*) and in a subpopulation of epithelial cells (*arrowheads*). Representative immunostaining with anti-SDF1 on +/+ stroma/+/+ epithelia and +/+ stroma/*Robo1*$^{-/-}$ epithelia. SDF1 immunostaining was scored and plotted on a vertical scatter plot. *Red bars,* average score. Significantly more SDF1 staining is seen in *Robo1*$^{-/-}$ outgrowths. ***, $P < 0.0001$, Mann-Whitney test. *Sdf1* mRNA is present in subpopulations of stromal fibroblasts (*b*; *open arrowheads*) and epithelial cells (*arrowheads*) in *Robo1*$^{-/-}$ outgrowths. *In situ* hybridization on +/+ stroma/+/+ epithelia and +/+ stroma/*Robo1*$^{-/-}$ epithelia outgrowths using antisense probes reveals *Sdf1* mRNA in +/+ stroma/*Robo1*$^{-/-}$ epithelia but not +/+ stroma/+/+ epithelia cells. Sense probes show little or no background staining. *Scale bar,* 20 μm.

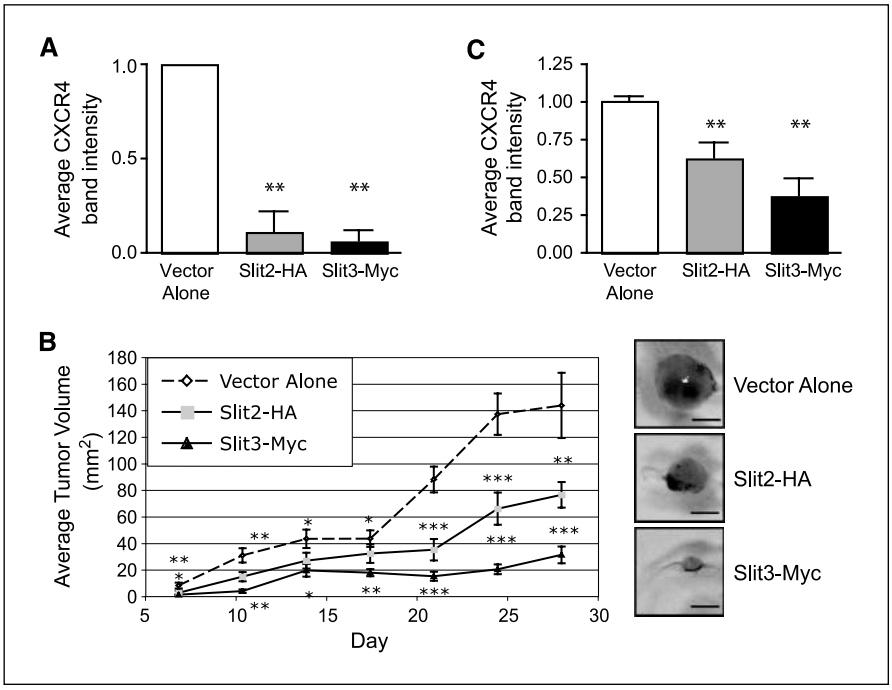

Figure 6. *Slit* expression in MDA-MB-231 cells blocks tumor growth by reducing CXCR4 expression. *A, Slit2*-HA and *Slit3*-Myc stable cell lines express low levels of CXCR4 compared with vector alone control lines. Stable *Slit2*-HA ($n = 3$) and *Slit3*-myc ($n = 2$) cell lines were generated by clonal selection. Stable cell line extracts were probed with anti-CXCR4. *Columns,* mean CXCR4 band intensity ($n = 2$ for each line); *bars,* SE. **, $P < 0.001$, ANOVA. *B,* expression of *Slit2* or *Slit3* resulted in smaller tumor size. Tumors were generated using *Slit* and control stable cell lines. $n = 12$ mice for each line. *Points,* mean tumor volume at each day; *bars,* SE. ***, $P < 0.0001$; **, $P < 0.001$; *, $P < 0.05$, ANOVA. Representative images of orthotopic tumors are shown. *Scale bar,* 0.25 mm. *C,* tumors expressing *Slit2* or *Slit3* contain significantly less CXCR4 protein compared with control tumors. *Columns,* mean CXCR4 immunoblot band intensity from $n = 3$ tumors; *bars,* SE. **, $P = 0.01$, ANOVA.

performed F4/80 immunohistochemistry on $Slit2^{-/-};Slit3^{-/-}$ and control tissue and found a significant increase in macrophages surrounding knockout tissue (Fig. 4*C, b*). We also evaluated the stromal expression of collagen, a major constituent of desmoplastic stroma (Fig. 4*C, c*). Stroma surrounding $Slit2^{-/-};Slit3^{-/-}$ epithelium contained significantly more condensed, collagenous stroma, compared with +/+, consistent with the histopathologic analysis. To define the cellular source of SDF1, we performed *in situ* hybridization analyses and discovered *Sdf1* in a fraction of epithelial cells and in a subset of elongated stromal cells that are likely to be fibroblasts based on their morphology (Fig. 4*D*). Thus, both CXCR4 and SDF1 are initially up-regulated in the epithelium, as has been recently observed in a xenograft model of DCIS (5). A local source of SDF1 may function to transform myoepithelial cells into CAFs or to recruit CAFs from circulating cells (35).

Epithelial regulation of CXCR4/SDF1 chemokine signaling axis. Together, the data show that loss of *Slit* expression leads to the coordinate up-regulation of *Cxcr4* in epithelia and *Sdf1* in both epithelia and stroma. This suggests that SLIT/ROBO1 signaling keeps SDF1/CXCR4 expression in check, but the regulatory networks may be complicated. *Slit* genes are expressed in the epithelia, but they encode a secreted cue that may act on any cell type expressing ROBO1 receptors. During mammary development, ROBO1 is expressed on myoepithelial cells (23), but as the gland matures, we observed a switch in its expression to include a subpopulation of luminal cells (Fig. 5*A*). ROBO1 was also expressed on stromal fibroblasts (Fig. 5*A*). Consequently, loss of *Slit* expression could regulate *Sdf1* and *Cxcr4* independently by disrupting ROBO1 signaling in both the stromal and epithelial compartments. Alternatively, loss of SLIT/ROBO1 signaling in just one compartment could up-regulate *Sdf1* and *Cxcr4* in both compartments.

To investigate, we eliminated SLIT/ROBO1 signaling selectively in the epithelial compartment by transplanting $Robo1^{-/-}$ epithelium into wild-type stroma. In these chimeric glands, we observed disorganized, hyperplastic epithelial lesions (Fig. 5*B*), which were similar in phenotype, penetrance (100%), and expressivity (19.64% ± SE 9.77; $n = 669$ ducts; 6 outgrowths) to those seen in $Slit2^{-/-};Slit3^{-/-}$ transplants (Fig. 1*A*). We evaluated the chemokine axis and again found up-regulation of CXCR4 in $Robo1^{-/-}$ epithelium (Fig. 5*C*), and coordinate up-regulation of SDF1 in the surrounding +/+ stroma (Fig. 5*D, a*), which was desmoplastic and contained immune infiltrates similar to stroma surrounding $Slit2^{-/-}Slit3^{-/-}$ tissue (data not shown). These data show that loss of SLIT/ROBO1 signaling in the epithelial compartment, alone, up-regulates SDF1 and CXCR4. This leads to phenotypic changes similar to those occurring in $Slit2^{-/-};Slit3^{-/-}$ transplants in which SLIT/ROBO1 signaling is disrupted in both compartments. To define the source of SDF1 in the transplanted tissue, we performed *in situ* hybridization studies and found *Sdf1* mRNA in cell subpopulations in the epithelia and stroma (Fig. 5*D, b*), suggesting that loss of SLIT/ROBO1 signaling in breast epithelia at early stages of transformation both generates a local source of *Sdf1* and up-regulates *Cxcr4*. We therefore conclude that loss of SLIT/ROBO1 signaling in the epithelia, alone, is sufficient to drive the observed morphologic and molecular changes, resulting in hyperplastic lesions, surrounded by desmoplastic stroma.

SLITs suppress CXCR4 expression and inhibit tumor growth. Given that SLITs exert this regulatory function by inhibiting the expression of *Sdf1* and *Cxcr4* within the mammary epithelium, we wondered whether overexpression of *Slits* in human breast carcinoma cells would suppress *Cxcr4* expression and inhibit tumor growth. Previous studies have shown that the metastatic human cell line MDA-MB-231 expresses CXCR4, but not SDF1 (36), and that inhibiting CXCR4 expression or function in these cells blocks primary tumor growth (8, 9). Because MDA-MB-231 cells express ROBO1 and ROBO2 (21),[4] signaling through these receptors could down-regulate CXCR4 expression and suppress tumor formation. To investigate, we transiently expressed *Myc-Slit2*

[4] R. Marlow, unpublished data.

or *Myc-Slit3* in MDA-MB-231 cells and documented decreased CXCR4 expression (Supplementary Fig. S4). Next, we generated stable cell lines expressing *Slit2* (n = 3) or *Slit3* (n = 2) and again found reduced CXCR4 levels (Fig. 6*A*). We also observed that *Slit*-expressing cells formed significantly fewer colonies, compared with control, when cultured in Matrigel (Supplementary Fig. S5). This suggested a general inhibition of cell growth, so we pursued the observation by establishing orthotopic xenograft tumors in immunocompromised hosts. We found that *Slit*-expressing cells formed significantly smaller tumors over time, with *Slit3* producing the most dramatic effect (Fig. 6*B*). We confirmed sustained down-regulation of CXCR4 in *Slit*-expressing tumors after 28 days of *in vivo* incubation (Fig. 6*C*; Supplementary Fig. S6). Thus, expression of *Slits* in MDA-MB-231 cells both down-regulates CXCR4 and inhibits tumor growth. Together with the observation that targeting CXCR4 reduces tumor growth in numerous organs (37, 38), our results suggest that SLITs suppress tumor growth by inhibiting the proliferative consequences of elevated CXCR4 expression.

Discussion

There is extensive literature on the molecular and genetic alterations that occur in invasive breast carcinoma and signify poor prognosis, but relatively little progress has been made in defining the genetic changes occurring in premalignant lesions. Here, we report that loss of *Slit* expression early during tumor progression up-regulates a key chemokine signaling axis and generates hyperplastic changes in the epithelium, along with desmoplastic changes in the stroma. Expression of CXCR4 was originally thought to occur late during tumor progression, generating cells that are ready to metastasize and home to organs expressing high levels of SDF1 (3). This restricted view of CXCR4 function, however, has been called into question because 93% of studied cases of atypical ductal carcinoma display high levels of CXCR4 (4), suggesting a role for CXCR4 in mediating earlier aspects of cellular transformation. Our data show that changes, loss and gain, in *Slit* expression function as a switch in the epithelium that up-regulate and down-regulate *Cxcr4*, leading to attendant changes in proliferation. We also show that loss of *Slits* results in the coordinate up-regulation of *Sdf1* in both the epithelium and surrounding stroma and this is accompanied by changes in the local microenvironment consistent with transformation.

The importance of the tumor microenvironment is well established, but it is unclear how it is generated. Our studies show that loss of SLIT/ROBO1 signaling exclusively in the epithelia is sufficient to increase expression of both *Cxcr4* and *Sdf1* (Fig. 5). The establishment of an initial SDF1/CXCR4 signaling loop within the epithelium is supported by recent studies using human MCF10DCIS.com cells in a xenograft model (5). Both CXCR4 and SDF1 are expressed at low levels in early MCF10DCIS lesions. CXCR4 expression remains epithelial, but during intermediate stages of transformation, SDF1 is switched on in the activated stroma. Once the ductal carcinoma becomes invasive, SDF1 expression is extinguished in the epithelia and is exclusively expressed by CAFs in the activated stroma. The origin of these CAFs is currently unknown. Some may be transformed from normal fibroblasts by aberrant signals from cancerous epithelial cells, whereas others may be transformed after being recruited from circulating bone marrow–derived cells (35). In either case, the transformation of these cells seems to be a consequence of their interaction with the cancerous epithelium. Our data raise the possibility that up-regulation of epithelial SDF1, accompanying *Slit* loss, contributes to the recruitment and/or transformation of CAFs, and support the model that genetic changes in the tumor epithelium, alone, are sufficient to drive transformation of cells and the surrounding microenvironment (7).

Our data also provide *in vivo* evidence that the SDF1/CXCR4 axis is fully functional within the epithelium during preinvasive stages of breast transformation and that it promotes cell survival and proliferation. We show that loss of SLIT/ROBO1 signaling results in the development of hyperplastic lesions (Fig. 1) with the coordinate up-regulation of both CXCR4 and SDF1 in the mammary epithelium (Figs. 2, 4, and 5). This type of autocrine stimulation of cell growth by SDF1/CXCR4 has been documented in human breast cancer cells on overexpression of SDF1 (39) and was also observed in the MCF10DCIS.com cells, described above, in which intraepithelial SDF1/CXCR4 signaling gives way to signaling across the epithelial/stromal boundary as the tumor microenvironment becomes established (5). Numerous pathways have been implicated in the mitogenic activity of SDF1/CXCR4 and may be responsible for the hyperplastic lesions observed in *Slit2*$^{-/-}$;*Slit3*$^{-/-}$ tissue (40). We are currently investigating the pathways that drive proliferation because targeting these pathways could provide therapies that arrest cellular proliferation in early stages of transformation.

The molecular mechanism through which cells acquire SDF1 and CXCR4 expression during the evolution of tumors is unclear. At later stages of cellular transformation, CXCR4 expression is up-regulated by several mechanisms (40). Our studies reveal a transcriptional mechanism during early stages of transformation that occurs within breast epithelia (Figs. 2, 4, and 5). We show that SLITs signal through their ROBO1 receptor to negatively regulate *Cxcr4* and *Sdf1*. Negative transcriptional regulation of both *Cxcr4* and *Sdf1* has been shown in renal cells where hypoxia-inducible factors 1 and 2 (Hif1 and Hif2) are targeted for degradation by von Hippel-Lindau (VHL) proteins (11). It has been shown that loss of VHL leads to stabilization of Hifs and subsequent up-regulation of both *Sdf1* and *Cxcr4* due to the Hif response elements contained in their promoters (41). Hifs are frequently up-regulated during breast transformation (42) and can drive the inappropriate proliferation of cells even under conditions of normal oxygen (43). Thus, Hifs or VHL proteins may be targeted by SLIT/ROBO1 signaling, and we are currently investigating their expression profiles in *Slit2*$^{-/-}$;*Slit3*$^{-/-}$ and *Robo1*$^{-/-}$ glands.

Numerous studies show epigenetic inactivation of *Slits* in multiple types of cancer (15, 16, 18, 19), and in breast, this loss of *Slit* also correlates with increasing tumor grade (44). Our histopathologic analyses of *Slit2*$^{-/-}$;*Slit3*$^{-/-}$ and *Robo1*$^{-/-}$ mammary epithelium revealed hyperplastic lesions with no nuclear atypia (Fig. 1), a type of lesion that can be found in ~30% of women with benign proliferative breast disease (45). Epidemiologic studies show that identification of such lesions confers a 2-fold increase in relative risk of developing invasive breast cancer compared with women without proliferative disease. For patients diagnosed with lesions having the next stage of severity, hyperplasias with nuclear atypia, the relative risk of future invasive disease rises to ~5-fold and increases to 10-fold if there is also positive family history (45, 46). These numbers show that, although most patients will not develop invasive disease, a fraction will. With medical advances enabling detection of breast lesions at earlier stages, it will be crucial to develop methods that distinguish between nascent disease and normal biology because current methods relying on

morphologic criteria are insufficient. Improved understanding of molecular signatures within breast lesions holds the promise of identifying those at high risk so they receive appropriate treatment while also identifying the majority who are not at risk so their medical concerns are dispelled (47). The findings presented in this report identify the loss of *Slit* expression as a marker of early lesions that have the potential to progress to invasive disease due to up-regulation of metastasis markers SDF1/CXCR4. We propose that these molecular alterations define a specific subclass of breast lesions whose early detection could lead to treatment strategies that prevent development of invasive disease.

Disclosure of Potential Conflicts of Interest

No potential conflicts of interest were disclosed.

Acknowledgments

Received 4/16/2008; revised 6/30/2008; accepted 7/25/2008.

Grant support: American Cancer Society grant RSG0218001MGO, California Breast Cancer Research Program grant 10PB-0188, and National Cancer Institute grant R01CA128902 (L. Hinck) and Congressionally Directed Medical Research Program grant BC043200 and National Cancer Institute grant U01 CA105490 (R.D. Cardiff).

The costs of publication of this article were defrayed in part by the payment of page charges. This article must therefore be hereby marked advertisement in accordance with 18 U.S.C. Section 1734 solely to indicate this fact.

Santa Cruz Biotechnology generously provided antibodies and siRNA reagents. Other generous gifts were the following: anti-Dutt1 (Dr. Rabbitts, University College, London, United Kingdom), anti-HA (Dr. Doug Kellogg), MCF7 and MDA-MB-231 cell lines (Dr. Bissell, Lawrence Labs, Berkeley, CA), pGL-CXCR4(−375) (Dr. Avraham, Harvard Medical School, Boston, MA), pCRII-SDF1 (Dr. Goffinet, University of Louvain Medical School, Brussels, Belgium), pRL-TK (Dr. Haussler, University of California, Santa Cruz, CA), pSecTagB-*hSlit3*-C-myc (Dr. Roy Bicknell), *Slit3*$^{-/-}$ mice (Dr. Ornitz, Washington University, St. Louis, MO), and *Slit2*$^{-/-}$ mice and *Robo1*$^{-/-}$ (Dr. Tessier-Lavigne, Genentech, Inc., South San Francisco, CA).

References

1. Salvucci O, Bouchard A, Baccarelli A, et al. The role of CXCR4 receptor expression in breast cancer: a large tissue microarray study. Breast Cancer Res Treat 2006;97:275–83.
2. Holm NT, Byrnes K, Li BD, et al. Elevated levels of chemokine receptor CXCR4 in HER-2 negative breast cancer specimens predict recurrence. J Surg Res 2007; 141:53–9.
3. Muller A, Homey B, Soto H, et al. Involvement of chemokine receptors in breast cancer metastasis. Nature 2001;410:50–6.
4. Schmid BC, Rudas M, Rezniczek GA, Leodolter S, Zeillinger R. CXCR4 is expressed in ductal carcinoma *in situ* of the breast and in atypical ductal hyperplasia. Breast Cancer Res Treat 2004;84:247–50.
5. Tait LR, Pauley RJ, Santner SJ, et al. Dynamic stromal-epithelial interactions during progression of MCF10DCIS.com xenografts. Int J Cancer 2007;120: 2127–34.
6. Orimo A, Gupta PB, Sgroi DC, et al. Stromal fibroblasts present in invasive human breast carcinomas promote tumor growth and angiogenesis through elevated SDF-1/CXCL12 secretion. Cell 2005;121:335–48.
7. Allinen M, Beroukhim R, Cai L, et al. Molecular characterization of the tumor microenvironment in breast cancer. Cancer Cell 2004;6:17–32.
8. Lapteva N, Yang AG, Sanders DE, Strube RW, Chen SY. CXCR4 knockdown by small interfering RNA abrogates breast tumor growth *in vivo*. Cancer Gene Ther 2005;12:84–9.
9. Smith MC, Luker KE, Garbow JR, et al. CXCR4 regulates growth of both primary and metastatic breast cancer. Cancer Res 2004;64:8604–12.
10. Helbig G, Christopherson KW, Bhat-Nakshatri P, et al. NF-κB promotes breast cancer cell migration and metastasis by inducing the expression of the chemokine receptor CXCR4. J Biol Chem 2003;278:21631–8.
11. Staller P, Sulitkova J, Lisztwan J, Moch H, Oakeley EJ, Krek W. Chemokine receptor CXCR4 downregulated by von Hippel-Lindau tumour suppressor pVHL. Nature 2003;425:307–11.
12. Lee BC, Lee TH, Zagozdzon R, Avraham S, Usheva A, Avraham HK. Carboxyl-terminal Src kinase homologous kinase negatively regulates the chemokine receptor CXCR4 through YY1 and impairs CXCR4/CXCL12 (SDF-1α)-mediated breast cancer cell migration. Cancer Res 2005;65:2840–5.
13. Li YM, Pan Y, Wei Y, et al. Upregulation of CXCR4 is essential for HER2-mediated tumor metastasis. Cancer Cell 2004;6:459–69.
14. Hinck L. The versatile roles of "axon guidance" cues in tissue morphogenesis. Dev Cell 2004;7:783–93.
15. Dallol A, Dickinson RE, Latif F. Epigenetic disruption of the SLIT-ROBO interactions in human cancer. In: Ablin RJ, Jiang WG, Esteller M, editors. DNA methylation, epigenetic and metastasis: New York: Springer Netherlands; 2005. p. 191–214.
16. Narayan G, Goparaju C, Arias-Pulido H, et al. Promoter hypermethylation-mediated inactivation of multiple Slit-Robo pathway genes in cervical cancer progression. Mol Cancer 2006;5:16.
17. Schmid BC, Rezniczek GA, Fabjani G, Yoneda T, Leodolter S, Zeillinger R. The neuronal guidance cue Slit2 induces targeted migration and may play a role in brain metastasis of breast cancer cells. Breast Cancer Res Treat 2007;106:333–42.
18. Latil A, Chene L, Cochant-Priollet B, et al. Quantification of expression of netrins, slits and their receptors in human prostate tumors. Int J Cancer 2003;103:306–15.
19. Sharma G, Mirza S, Prasad CP, Srivastava A, Gupta SD, Ralhan R. Promoter hypermethylation of p16INK4A, p14ARF, CyclinD2 and Slit2 in serum and tumor DNA from breast cancer patients. Life Sci 2007;80:1873–81.
20. Wu JY, Feng L, Park HT, et al. The neuronal repellent Slit inhibits leukocyte chemotaxis induced by chemotactic factors. Nature 2001;410:948–52.
21. Prasad A, Fernandis AZ, Rao Y, Ganju RK. Slit protein-mediated inhibition of CXCR4-induced chemotactic and chemoinvasive signaling pathways in breast cancer cells. J Biol Chem 2004;279:9115–24.
22. Chalasani SH, Sabelko KA, Sunshine MJ, Littman DR, Raper JA. A chemokine, SDF-1, reduces the effectiveness of multiple axonal repellents and is required for normal axon pathfinding. J Neurosci 2003;23:1360–71.
23. Strickland P, Shin GC, Plump A, Tessier-Lavigne M, Hinck L. Slit2 and netrin 1 act synergistically as adhesive cues to generate tubular bi-layers during ductal morphogenesis. Development 2006;133:823–32.
24. Robinson GW, Accili D, Hennighausen L. Rescue of mammary epithelium of early lethal phenotypes by embryonic mammary gland transplantation as exemplified with insulin receptor null mice. New York: Kluwer Academic/Plenum Press; 2000. p. 307–16.
25. Srinivasan K, Strickland P, Valdes A, Shin GC, Hinck L. Netrin-1/neogenin interaction stabilizes multipotent progenitor cap cells during mammary gland morphogenesis. Dev Cell 2003;4:371–82.
26. Silberstein GB, Daniel CW. Investigation of mouse mammary ductal growth regulation using slow-release plastic implants. J Dairy Sci 1987;70:1981–90.
27. Tissir F, Wang CE, Goffinet AM. Expression of the chemokine receptor Cxcr4 mRNA during mouse brain development. Brain Res Dev Brain Res 2004;149:63–71.
28. Lee GY, Kenny PA, Lee EH, Bissell MJ. Three-dimensional culture models of normal and malignant breast epithelial cells. Nat Methods 2007;4:359–65.
29. Bartoe JL, McKenna WL, Quan TK, et al. Protein interacting with C-kinase 1/protein kinase Cα-mediated endocytosis converts netrin-1-mediated repulsion to attraction. J Neurosci 2006;26:3192–205.
30. Wu X, Chen H, Parker B, et al. HOXB7, a homeodomain protein, is overexpressed in breast cancer and confers epithelial-mesenchymal transition. Cancer Res 2006;66:9527–34.
31. Dallol A, Da Silva NF, Viacava P, et al. SLIT2, a human homologue of the *Drosophila Slit2* gene, has tumor suppressor activity and is frequently inactivated in lung and breast cancers. Cancer Res 2002;62:5874–80.
32. Richardson AL, Wang ZC, De Nicolo A, et al. X chromosomal abnormalities in basal-like human breast cancer. Cancer Cell 2006;9:121–32.
33. Holland JD, Kochetkova M, Akekawatchai C, Dottore M, Lopez A, McColl SR. Differential functional activation of chemokine receptor CXCR4 is mediated by G proteins in breast cancer cells. Cancer Res 2006;66:4117–24.
34. Lin EY, Li JF, Gnatovskiy L, et al. Macrophages regulate the angiogenic switch in a mouse model of breast cancer. Cancer Res 2006;66:11238–46.
35. Orimo A, Weinberg RA. Stromal fibroblasts in cancer: a novel tumor-promoting cell type. Cell Cycle 2006;5: 1597–601.
36. Kang H, Watkins G, Parr C, Douglas-Jones A, Mansel RE, Jiang WG. Stromal cell derived factor-1: its influence on invasiveness and migration of breast cancer cells *in vitro*, and its association with prognosis and survival in human breast cancer. Breast Cancer Res 2005;7:R402–10.
37. Rubin JB, Kung AL, Klein RS, et al. A small-molecule antagonist of CXCR4 inhibits intracranial growth of primary brain tumors. Proc Natl Acad Sci U S A 2003; 100:13513–8.
38. De Falco V, Guarino V, Avilla E, et al. Biological role and potential therapeutic targeting of the chemokine receptor CXCR4 in undifferentiated thyroid cancer. Cancer Res 2007;67:11821–9.
39. Kang H, Mansel RE, Jiang WG. Genetic manipulation of stromal cell-derived factor-1 attests the pivotal role of the autocrine SDF-1-CXCR4 pathway in the aggressiveness of breast cancer cells. Int J Oncol 2005;26:1429–34.
40. Luker KE, Luker GD. Functions of CXCL12 and CXCR4 in breast cancer. Cancer Lett 2006;238:30–41.
41. Zagzag D, Krishnamachary B, Yee H, et al. Stromal cell-derived factor-1α and CXCR4 expression in hemangioblastoma and clear cell-renal cell carcinoma: von Hippel-Lindau loss-of-function induces expression of a ligand and its receptor. Cancer Res 2005;65:6178–88.
42. Zhong H, De Marzo AM, Laughner E, et al. Overexpression of hypoxia-inducible factor 1α in common human cancers and their metastases. Cancer Res 1999; 59:5830–5.
43. Dang DT, Chen F, Gardner LB, et al. Hypoxia-inducible factor-1α promotes nonhypoxia-mediated proliferation in colon cancer cells and xenografts. Cancer Res 2006;66:1684–936.
44. Miller LD, Smeds J, George J, et al. An expression signature for p53 status in human breast cancer predicts mutation status, transcriptional effects, and patient survival. Proc Natl Acad Sci U S A 2005;102:13550–5.
45. Hartmann LC, Sellers TA, Frost MH, et al. Benign breast disease and the risk of breast cancer. N Engl J Med 2005;353:229–37.
46. Fitzgibbons PL, Henson DE, Hutter RV. Benign breast changes and the risk for subsequent breast cancer: an update of the 1985 consensus statement. Cancer Committee of the College of American Pathologists. Arch Pathol Lab Med 1998;122:1053–5.
47. Jeffrey SS, Pollack JR. The diagnosis and management of pre-invasive breast disease: promise of new technologies in understanding pre-invasive breast lesions. Breast Cancer Res 2003;5:320–8.